INTERACTION OF *E.COLI* AND AUTOCHTHONOUS RIVER WATER MICROORGANISMS WITH POLYMERS IN HEAT TRANSFER APPLICATIONS

S. Pohl[1], M. Madzgalla[2], W. Manz[2] and H.-J. Bart[1]

[1] University of Kaiserslautern, Chair of Separation Science and Technology, Kaiserslautern/Germany
E-mail (bart@mv.uni-kl.de)
[2] University of Koblenz-Landau, Institute of Integrated Natural Sciences - Microbiology, Koblenz/Germany

ABSTRACT

The biofouling affinity of various polymeric surfaces (polypropylene, polysulfone, polyethylene terephthalate, polyether ether ketone) was studied using native biofilms originating from the rivers Rhine and Moselle and the model bacterium *E.coli* K12 DSM 498 in polymeric plate heat exchanger applications and compared with the industrial standard stainless steel 304. Polymers with low apolar surface free energy of 25.29-27.91 mN m^{-1} and significant electron-donating, but no electron-accepting fractions of the surface free energy were found to resist biomass deposition of both microorganism systems most efficiently, a fact being verified by DLVO calculations. The required shear stress in order to remove already formed biofilms was found to be lowest on polymers with 9-19 N m^{-2}, which was investigated by using a rotating disk in water with fixed samples (Fowler cell). The adhesion forces seemed to be linked to the acid-base component of the surface free energy, being lowest on apolar surfaces.

INTRODUCTION

Biofouling, as the unwanted settlement of bacteria, algae and macroorganisms like mollusks, and the inherent forming of various excreted extracellular polymeric substances (EPS) (Roosjen et al. 2004) is a large problem in medical, food packaging, marine and industrial applications (Banerjee et al. 2011). The microorganism-specific EPS composition hereby consists of various proteins, polysaccharides, lipids or long-chain carbohydrates in general. Usage of untreated river water in industrial heat exchangers will also cause biofouling, which in return results in an additional heat transfer resistance decreasing the overall heat exchanger efficiency and increases the required pump capacity due to increased friction and reduction of the inner diameter of tubing and flow channels in heat exchangers (Steinhagen et al. 1993). The resulting moderate temperatures throughout all the different process sections, like tubing, heat exchangers and cooling towers, can enhance the biofouling process. Heat exchanger oversizing, heat loss, increased required pump capacity and higher maintenance costs are the resulting fouling related costs.

The choice of a certain polymeric material in heat exchanger applications is strongly linked to its promising bacterial adhesion properties and the ability to withstand corrosion induced by metabolic processes in the biofilm matrix. Heat exchangers utilizing thin polymeric films as heat transfer surfaces could therefore vastly increase the efficiency of heat transfer processes in environments characterized by high microbial loads and simultaneously provide sufficient heat transfer coefficients by using polymer film thicknesses of 25-50 µm. As the respective polymer films were already found to have a low crystallization fouling affinity (Dreiser et al., 2015), extended investigations concerning biofouling were conducted. The investigations focused on two steps in order to describe the influence of replacing stainless steel surfaces with polymer films in plate heat exchanger applications: (i) reduction of the governing process of initial microorganism adhesion to the surface; (ii) investigation of the shear force necessary to detach the already formed biofilms in order to estimate the adhesion force between biofilm and the respective surfaces. These critical shear forces is a basis to implement cleaning in place techniques to overcome adhesion forces of the biofilms and therefore provide a surface with little or no thermal fouling resistance.

EXPERIMENTAL

Materials and Preparation

The tendency towards biofouling of the polymers was compared to that of stainless steel 304 (SS). Two polyether ether ketones (PEEK, one semi-crystalline, one additionally filled with 30% talcum), two polysulfones (PSU, one ut: untreated, one ct: corona-treated), polypropylene (PP) untreated and polyethylene terephthalate (PET) ut were selected as polymers. The stainless steel surface was cold-milled but otherwise untreated. Prior to use all surfaces were cleansed with deionized (DI) water.

Escherichia coli K12 DSM 498 was chosen as model bacterium due to its safe and simple usage and the fact that these microorganisms do not develop cell appendages that could alter the interaction process. Samples of river water from Rhine and Moselle were taken at a location near Koblenz, Germany, a few kilometers apart mid-March 2016.

Fouling experiments concerning the general fouling tendency were conducted in a system of seven parallel flow channels that were operated with a peristaltic pump. The

ISBN: 978-0-9984188-0-3; Published online www.heatexchanger-fouling.com

channels were arranged vertically in order to diminish the effects of sedimentation and the pulsation of the peristaltic pump was eliminated by using separate water filled pressure vessels prior to the channel entrances. A schematic of the flow channels including an optional weir for better liquid dispersion at low flow rates and the possibility to specifically heat the substrata via a separate heating agent circuit as described elsewhere (Pohl et al., 2015a). The channels were machine-cut and had an inner length of 12 cm and width of 3 cm. The channel height was 1 cm and resembles typical distances between plates in plate heat exchangers. The entrance and outlet length of 2 cm were shaped in the form of a trapezium, in order to provide parallel flow profiles in the middle investigation section.

The preparatory *E.coli* microorganisms were cultivated with 1 L of LB-Miller nutrient solution (10 g L^{-1} NaCl, 10 g L^{-1} tryptone and 5 g L^{-1} yeast extract) at 37°C in a shaking bath at 120 rpm for 24 h. The next day 50 mL of this preparatory culture was transferred into 1 L of 1:10 diluted LB medium, as this dilution prove to provide the most stable cell concentrations over the experiment duration (Pohl et al., 2015b). This batch was then subsequently used as feed for the flow channels after the optical density (OD) reached 0.6, which was constantly monitored via regular measurements with a photometer (Lambda Bio+, PerkinElmer), and resembles approximately 10^8 cells mL^{-1}. The autochthonous microorganisms were cultivated accordingly, but a standard R2a nutrient solution was used in order to simultaneously grow all inherent microorganisms of the river samples at a comparable cell concentration.

The experiments were conducted multiple times over 3 days and once over 44 days, whilst for the long-term experiment the batch feed was changed every 7 days in order to prevent growth equilibria due to degeneration of the microorganisms.

The experiments were operated at 100 ml min^{-1} per channel in a recirculating mode into the batch and in preceding CFD simulations these flow rates calculated to result in $Re \approx 110$ near the surface of the middle section and so laminar flow was assumed. This laminar flow was chosen, as solely the influence of the surface properties of substrata and microorganisms should be dominant and fluid forces diminished. By minimizing the influence of removal processes, the total biomass on the substrata can be directly correlated to the respective surface properties.

Bacterial cell counts were determined by epi-fluorescence microscopy (staining SYBR Green I) over the investigated biofilm area in the middle section of the flow channels in order to reduce the effects of the flow at the inlet, outlet and wall region. Five fields of view with an area of 0.02 mm^2 were randomly selected for every sample.

Surface properties

The surface properties that were determined and further investigated both for the microorganisms and substrata, were the surface free energy and zeta potential as preceding investigations showed the influence of substrata roughness to be negligible compared to the influence of surface free energy (Pohl et al., 2015b, Pohl et al., 2017). The surface free energies were obtained by measuring the contact angles of 4 different test liquids (DI water, diiodomethane, formamide and ethylene glycol).

The contact angles θ of every test liquid correlates with the surface free energies of the substrate according to the Young's equation and depends on the thermodynamic equilibrium of the participating phases of solid s, liquid l and vapor phase v:

$$\gamma_{lv} \cos\theta = \gamma_{sv} - \gamma_{sl} \quad (1)$$

According to the acid base theory, the surface free energy of the solid-liquid interface can be calculated by using Eq. (2) (van Oss, 1995).

$$\gamma_{sl} = \left(\sqrt{\gamma_{sv}^{LW}} - \sqrt{\gamma_{lv}^{LW}}\right)^2 + 2\left(\sqrt{\gamma_{sv}^{+}\gamma_{sv}^{-}} + \sqrt{\gamma_{lv}^{+}\gamma_{lv}^{-}} - \sqrt{\gamma_{sv}^{+}\gamma_{lv}^{-}} - \sqrt{\gamma_{sv}^{-}\gamma_{lv}^{+}}\right) \quad (2)$$

In order to acquire the respective surface free energy fractions of apolar Lifshitz-van der Waals γ_{sv}^{LW}, electron donor γ_{sv}^{-} and electron acceptor γ_{sv}^{+}, contact angle measurements of at least 3 different liquids, of which at least 2 must be polar, have to be conducted. The system of equations can then be solved using Eq. (3) for each liquid and its respective mean contact angle θ.

$$(1+\cos\theta)\cdot\gamma_{lv} = 2\left(\sqrt{\gamma_{sv}^{LW}\gamma_{lv}^{LW}} + \sqrt{\gamma_{sv}^{+}\gamma_{lv}^{-}} + \sqrt{\gamma_{sv}^{-}\gamma_{lv}^{+}}\right) \quad (3)$$

Contact angles for the microorganisms were determined on stable microbial lawns. These cell layers were obtained by centrifuging 200 mL of the bacterial suspension at 8000 g for 5 minutes and washed twice with potassium phosphate magnesium sulfate buffer solution (PPMS: 6.97 g K2HPO4, 2.99 g KH2PO4 and 0.2 g MgSO4·7 H2O per liter DI water), which was adjusted to pH = 7. This washing process was used in order to diminish the effects the nutrient solution on the contact angle and zeta potential measurement (Wilson et al. 2001). The residual washing solution was pipetted and the remaining bacterial cells were homogeneously spread onto glass slides. After 30 min in the desiccator to remove most excess liquid between cells, the contact angles of all liquids remained stable on the bacterial lawns.

The surface zeta potential was measured using an Electro Kinetic Analyzer (Anton Paar GmbH, Graz, Germany) with automatic titration unit for varying pH values and rectangular measuring channel. The electrolyte solution was 10^{-3} M KCl which is standard for calculating surface zeta potentials and attributed via the measuring software, pH variation was 0.1 M HCl and 0.1 M KOH and the channel height was 500 µm, whilst the length was 80 mm and the channel surface area was 5 mm^2.

The zeta potential of the *E.coli* and the native microorganisms obtained from the rivers Rhine and Moselle were measured using a Zetasizer Nano Z (Malvern Instruments Ltd, Worcestershire, UK) via their electrokinetic mobility. The *E.coli* microorganisms and the autochthonous river water microflora were cultivated for 24 h and 72 h in LB Miller medium and R2a medium, respectively. The obtained cell suspensions were subsequently centrifuged at

8000 g for 5 min and washed twice with PPMS buffer adjusted to pH of 7 and half of the sample was immersed in PPMS and the other in DI water. The measured liquid properties viscosity, refraction index and electrochemical properties of PPMS and DI water were used for the calculation of the bacterial zeta potential for both liquids.

Fouling resistance

In order to correlate the interaction of the surface characteristics of substrata and the microorganisms, both the dry biomass as indicator for the excreted biomass and the cell numbers for direct cell-surface interaction were investigated over the experimental durations of 3 and 44 days for each substratum. The biomass m_f is especially interesting, as the resulting fouling resistance R_f in thermal systems strongly correlates with the biofilm thickness x_f, biofilm density ρ_f, thermal conductivity λ_f (Eq. (4)) and therefore the mean biomass across the surface A_f. The fouling resistance R_f can therefore be expressed as the overall heat transfer of the clean surface U_0 to that of the surface with fouling U_f.

$$R_f = \frac{1}{U_f} - \frac{1}{U_0} = \frac{x_f}{\lambda_f} = \frac{m_f}{\rho_f \cdot A_f \cdot \lambda_f} \tag{4}$$

Fouling experiments with autochthonous microorganisms were solely conducted with Rhine microorganisms, due to the similarity of their inherent surface characteristics.

DLVO/X-DLVO Theory

Assuming an irreversible adhesion for net attraction without the influence of shear forces, the distance dependent interaction of a spherical particle or microorganism and a surface in the DLVO theory (based on the work of Derjaguin and Landau (1941) and Verwey and Overbeek (1948)) is commonly described as the balance of attractive Lifshitz-van der Waals energies, attractive or repulsive electrostatic energies and, in the case of the extended DLVO (X-DLVO) theory, attractive or repulsive acid-base interaction energies (van Oss et al. 1985). The extension of polar forces was introduced in order to describe close-range anomalies like hydrophobic attraction and hydrophilic repulsion. The resulting distance-dependent total interaction energy G_{total} can be expressed as the sum of the separate interaction energies of apolar Lifshitz-van der Waals G^{LW}, polar acid-base G^{AB} and electrostatic G^{EL} fractions (Eq. (5)).

$$G_{total}(d) = \mathrm{G}^{LW}(d) + \mathrm{G}^{AB}(\mathrm{d}) + G^{EL}(d) \tag{5}$$

The Lifshitz-van der Waals component for sphere-plate interaction, which is a model for the initial adhesion of a single microorganism with a defined semi-infinite flat and smooth surface can be calculated by utilizing the Hamaker constant A_H, the mean bacteria radius r and the separation distance d (Eq. (6)):

$$G^{LW}(d) = -\frac{A_H}{6}\left[\frac{r}{d} + \frac{r}{d+2r} + \ln\left(\frac{d}{d+2r}\right)\right] \tag{6}$$

According to the DLVO theory, the Hamaker constant A_H can be calculated by a combination of thermodynamic and classical DLVO approaches (Eq. (7)) (Bos et al. 1999) and can be obtained from the Lifshitz-van der Waals adhesion energy $\Delta G_{adh}{}^{LW}$ (Eq. (8)), which is derived from contact angle measurements, and the distance of closest approach d_0 which is 1.53 Å. The Lifshitz-van der Waals adhesion energy is negative for almost all microbial interactions, implying predominantly attractive Lifshitz-van der Waals interaction forces (Bos et al. 1999).

$$A_H = -12\pi d_0^2 \Delta G_{adh}^{LW} \tag{7}$$

$$\Delta G_{adh}^{LW} = -2\left(\sqrt{\gamma_{mv}^{LW}} - \sqrt{\gamma_{lv}^{LW}}\right)\left(\sqrt{\gamma_{sv}^{LW}} - \sqrt{\gamma_{lv}^{LW}}\right) \tag{8}$$

The Lifshitz-van der Waals adhesion energy between microorganism and substratumis therefore solely dependent on the respective apolar surface free energies of liquid l, microorganism m and substratum s.

The acid-base component G^{AB} (Eq. (9)) of the total interaction energy can be acquired from the acid-base adhesion energy $\Delta G_{adh}{}^{AB}$ (Eq. (10)), which also includes the surface free energies based on contact angle measurements. In Eq. (9), λ denotes the correlation length of molecules in a liquid medium, which can be 0.6 – 1 nm for hydrophilic repulsion, but can also reach a dimension of 13 nm and more for larger distances (d > 10 nm) between particle and surface (van Oss 1995). The acid-base adhesion energy therefore depends on the combination of electron-donating and –accepting surface free energy components.

$$G^{AB}(d) = 2\pi r\lambda\Delta G_{adh}^{AB} \cdot \exp\left(\frac{d_0 - d}{\lambda}\right) \tag{9}$$

$$\Delta G_{adh}^{AB} = 2\left[\begin{array}{l}\left(\sqrt{\gamma_{mv}^{+}} - \sqrt{\gamma_{sv}^{+}}\right)\left(\sqrt{\gamma_{mv}^{-}} - \sqrt{\gamma_{sv}^{-}}\right) - \left(\sqrt{\gamma_{mv}^{+}} - \sqrt{\gamma_{lv}^{+}}\right)\cdot \\ \cdot\left(\sqrt{\gamma_{mv}^{-}} - \sqrt{\gamma_{lv}^{-}}\right) - \left(\sqrt{\gamma_{sv}^{+}} - \sqrt{\gamma_{lv}^{+}}\right)\left(\sqrt{\gamma_{sv}^{-}} - \sqrt{\gamma_{lv}^{-}}\right)\end{array}\right] \tag{10}$$

The electrostatic interaction energy G^{EL} (Eq. (11)) is thereby a function of the zeta potentials ζ of the bacterial cell and the surface, the ion-dependent double layer thickness κ^{-1} (Eq. (12)) and the dielectric constant ε of the liquid medium.

$$G^{EL}(d) = \pi\varepsilon r\left(\zeta_1^2 + \zeta_2^2\right)\left[\frac{2\zeta_1\zeta_2}{\zeta_1^2 + \zeta_2^2} \cdot \ln\frac{1+\exp(-\kappa d)}{1-\exp(-\kappa d)} + \ln\left\{1-\exp(-2\kappa d)\right\}\right] \tag{11}$$

$$\kappa = \sqrt{\left(\frac{e}{\varepsilon kT} \cdot \sum_i z_i \cdot n_i\right)} \tag{12}$$

In Eq. (12), e denotes the electron charge, k the Boltzmann constant, T the temperature, z_i the valency of the ions present and n_i the number of ions per unit volume.

Adhesion forces

Measuring the adhesion forces between single microorganisms or complete biofilms is difficult due to the viscous behavior of the biofilms and the impossibility to

attach probes to those whole biofilm samples. Therefore numerous continuous liquid flow methods were invented in order to vary the fluid velocities above the sample surfaces and so generate different shear forces acting on the fouling layers. A comparison was given by Bos et al. (1999) with methods reaching from flow channels, stagnation point flow, slides and rotating disks, that are still used today.

The rotating disk in a stagnating liquid, which was investigated by Fowler and McKay (1980), was chosen as screening method, as it was easy and biofilm preserving to use the sample surface from the continuous fouling experiments described above and fix them onto the disk surface with double sided adhesive tape (Fig. 1).

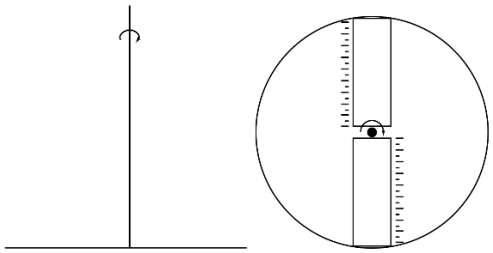

Fig. 1: Horizontal rotating disk setup in static liquid (left) and the position of two sample surfaces on the disk (right)

The general idea behind the rotating disk is that due to the rotation of the disk, a defined fluid induced shear force is present at each point in relation to the distance from the central shift. If the shear forces excel the adhesion forces at a given point, a clear detachment line should be visible. This detachment line would then move towards the central axis by increasing the rotational speed but should result in identical detachment shear forces. Under these conditions, the wall shear stress τ would vary linearly (Eq. (13)) with the radial position according to García et al. (1997) for laminar flow conditions of $Re < 3\ 10^5$ (Schlichting et al. 2000) defined in Eq. (14).

$$\tau = 0.8r\sqrt{\rho\eta\omega^3} \tag{13}$$

$$Re = \frac{r_d^2\omega\rho}{\eta} \tag{14}$$

In Eq. (13) and Eq. (14) ω is defined as the rotational speed of the disk, η as the dynamic viscosity of the stagnant fluid and r_d as the radius of the disk.

The experiments were conducted with *E.coli* microorganisms after 2 weeks with laminar flow conditions on at least two samples of every surface, except for PSU ct, and investigated for at least 6 different rotational speeds between about 15 and 52 rad s^{-1} for 1 minute. The radius of the disk was 0.125 m.

RESULTS & DISCUSSION

Surface properties

The calculated surface free energy compositions of the substrata according to sessile drop techniques are depicted in Table 1.

Table 1. Surface free energies and their composition for the investigated substrata (mN m^{-1})

Material	γ_{sv}^{LW}	γ_{sv}^{+}	γ_{sv}^{-}
PSU ut	27.88	0	14.35
PP ut	25.98	0.06	1.05
PEEK(filler) ut	33.26	2.20	4.98
PEEK ut	39.59	0	3.65
PSU ct	41.91	0.05	19.70
PET ut	41.91	0	6.35
SS 304	37.15	0	5.80

Table 1 shows, that for most substrata, the electron donor fraction exceeds the electron acceptor fractions, which in return leads to an overall mostly apolar or weak polar charge (acid-base component, AB) of the substrata (Eq. (15)) and so the apolar Lifshitz-van der Waals component dominates the polymer and stainless surface free energies.

$$\gamma_i^{AB} = 2\sqrt{\gamma_i^+\gamma_i^-} \tag{15}$$

Fig. 2 shows a comparison of the respective substrata concerning their pH dependency. The titration volume of both the acid and base was 0.2 mL, the measurement was repeated 6 times at each pH value in both streaming directions. The differences in the pH steps for some surfaces is related to material swelling and buffer capacity of the surfaces (Luxbacher 2014).

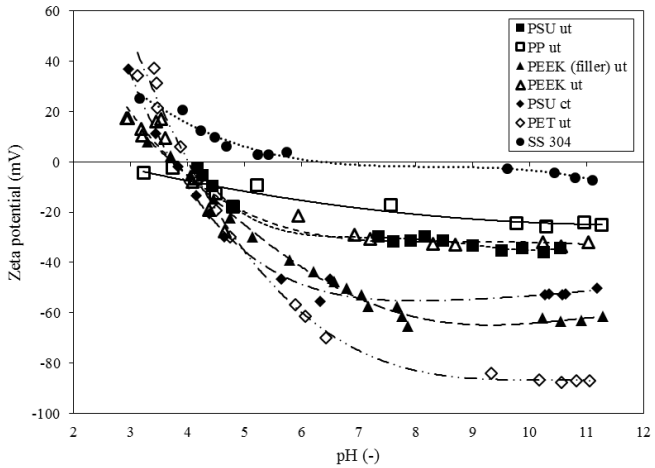

Figure 2: pH-dependent zeta potential of the respective polymers and SS 304

All surfaces are negatively charged for common pH values of native river water (pH 5 to 9), and in combination with the negative surface charge of the bacteria electrostatic repulsion is dominant. The exception is SS 304, which has its isoelectric point (IEP) at pH 6.5 to 7 and has a comparatively high zeta potential at pH values above 7. The isoelectric point of the polymer surfaces is around a pH of 4.

The surface free energies of the microorganisms *E.coli* K12 DSM498, Rhine and Moselle are depicted in Table 2. The data from Table 2 shows, that the microorganisms have a high fraction of electron donator in the surface free energy, which especially for the non-zero autochthonous microorganisms of Rhine and Moselle results in a significant

polar fraction of the surface free energy according to Eq. (15). The conformity between Rhine and Moselle microorganisms can be explained by the spatial proximity of the sample locations of the two rivers at Koblenz and the poor mixing of the rivers that can be seen in photographs of the inflow at certain seasons.

Table 2. Surface free energies and their composition for the investigated microorganism systems *E.coli* K12 DSM 498, Rhine and Moselle (mN m^{-1})

Microorganism	γ_{sv}^{LW}	γ_{sv}^{+}	γ_{sv}^{-}
E.coli K12	29.40	0	139.91
Rhine	34.91	0.88	39.82
Moselle	35.16	0.84	41.99

The calculated zeta potential of *E.coli* at pH = 7 with -51.52±1.83 mV in DI water is in good accordance to findings of Soni et al. (2007) which was -47.8 mV. The zeta potential of *E.coli* in PPMS, which has comparable ion molarities of the fouling experiments, was calculated to be -15.2 mV and shows the high influence of ions on the electrostatic interaction. Interestingly, the data of the rivers Rhine with -25.61 ± 1.20 mV and Moselle with -23.93 ± 1.80 mV in DI water, showed relatively low standard deviations concerning zeta potentials.

Biomass quantity

As can be seen from Table 3, the resulting mean dry biomass and mean cell numbers after 3 days show opposing trends for most polymers with the exception of PSU ct. This phenomenon could be linked to the naturally occurring quorum sensing effect depending strongly on cell density (Tan et al. 2014), especially in monospecies biofilms, but was not further investigated in this work.

Table 3: Mean dry biomass *m* (mg) and mean cell numbers *n* of *E.coli* K12 for each substratum after 3 and 44 days

Material	$m_{E.coli}(3d)$	$n_{E.coli}(3d)$	$m_{E.coli}(44d)$
PSU ut	5.84	3108	33.20
PP ut	5.86	3080	23.96
PEEK(filler) ut	7.70	1664	10.32
PEEK ut	9.37	604	13.10
PSU ct	9.83	2239	25.96
PET ut	13.34	602	7.98
SS 304	17.39	-	29.75

The cell numbers on SS 304 could not be evaluated. Polymers showed clear advantage against SS 304 concerning biomass over 3 days, whilst for the long-term experiments, polymers with initially lower biomass but high cell numbers consecutively resulted in a higher biomass partly even exceeding the biomass of SS 304. Solely PEEK ut, PEEK (filler) ut and PET ut, with initially low cell numbers, also showed less biomass after 44 days, which could be related to a delayed excretion of EPS per cell and could therefore explain the high biomass for surfaces with high cell numbers.

An experimental duration of 3 days revealed a strong significant difference in the p-value of the cell counts of *E.coli* on polymers p_{cell} (*E.coli*, polymers) = $2.143 \cdot 10^{-7}$. However, the difference in the dry biomass of *E.coli* on polymers with $p_{biomass}$ (*E.coli*, polymers) = 0.715 was not significant (Pohl et al. 2015b). In other words, due to the higher variance no distinct deviation could be made between the polymers without knowledge of the surface chemistry. A more detailed investigation of the surface free energy, which is of high significance revealed similar biomass deposition for similar surface free energies (see Table 1 and Table 3).

Table 4: Mean dry biomass *m* (mg) and mean cell numbers *n* of Rhine microorganisms for each substratum after 3 and 44 days

Material	$m_{Rhine}(3d)$	$n_{Rhine}(3d)$
PSU ut	1.30	1940
PP ut	1.40	1772
PEEK(filler) ut	1.47	1580
PEEK ut	1.03	1173
PSU ct	1.30	1111
PET ut	1.60	1409
SS 304	12.80	1044

Table 4 revealed similar effects for Rhine micro-organisms, where the p-value of Rhine microorganisms on polymers is p_{cell} (Rhine, polymers) = 0.801 respectively $p_{biomass}$ (Rhine, polymers) = 0.761 and shows no significance due to the higher variance and the similarity of results between distinct substrata. Concerning the relation of biomass or cell numbers to the surface characteristics of the substrata, no clear statistical or causal connections could be observed.

According to investigations of Baier (1980), the optimal surface free energy for which microbial adhesion is minimal is about 25 mN m^{-1}. Surface free energies smaller or bigger than 25 mN m^{-1} would result in an increased relative bacterial adhesion. These findings were correlated by Zhao et al. (2005) into the following equation, which calculates the optimal surface free energy for preventing the adherence of microorganisms to a surface.

$$\gamma_{sv}^{opt} = \gamma_{sv}^{LW} = \frac{1}{4}\left(\sqrt{\gamma_{mv}^{LW}} + \sqrt{\gamma_{lv}^{LW}}\right) \quad (16)$$

Equation (16) assumes, that most surfaces have little or no electron-donating component γ_{sv}^{+} and therefore the interaction of microorganism and surface is dominated by apolar Lifshitz-van der Waals forces. The validity of the findings concerning little electron-donating fraction of the surface free energy can be seen in Table 1. The optimal surface free energy of the substrata can therefore be calculated based on the surface free energies of the immersion liquid (in this case water) and the micro-organisms. Combining Eq. (16) with the data of Table 2, the optimal surface free energy would be 25.29 mN m^{-1} for *E.coli* K12, 27.80 mN m^{-1} for Rhine microorganisms and 27.91 mN m^{-1} for Moselle microorganisms. These findings, especially for *E.coli*, correlate well with the dry biomass of Table 3 and therefore support the investigations of Baier (1980).

ISBN: 978-0-9984188-0-3; Published online www.heatexchanger-fouling.com

DLVO/X-DLVO Theory

Fig. 3 shows the calculated distance dependent interaction energies between *E.coli* K12 and the investigated surfaces at pH = 7 and ion concentrations according to the fouling experiment of 0.171 M using data of Tables 1 and 2. The scale of the Brownian motion energy of a one single organism [$1\ kT = 4.11 \cdot 10^{-21}$ J] is commonly taken as energy scale and provides therefore reference for the adhesion process. Comparing results of Fig. 3 with the data of Table 3 it becomes obvious, that the dry biomass strongly depends on the apolar Lifshitz-van der Waals fraction of the surface free energy and directly correlates with it for the polymer surfaces. For SS 304 this clear trend could not be seen in the calculations due to the strong repulsive influence of acid-base forces in the wall-near region.

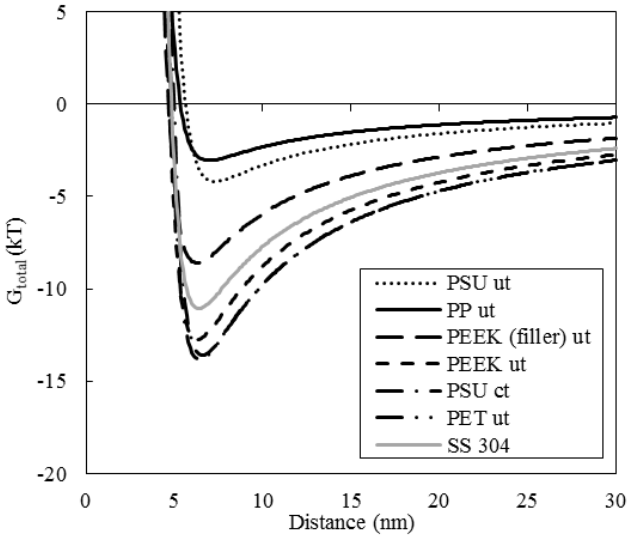

Fig. 3: Distance dependent interaction energies (X-DLVO) between *E.coli* K12 and the respective substrata, with ion molarities of 0.171 M according to the laboratory experiment at pH = 7

When applying the classical DLVO theory without the influence of acid-base interactions (see Fig. 4) it can be seen, that whilst the trend for the polymer surfaces remains intact, the strong attractive forces of electrostatic and apolar forces for the SS 304 now also fits the excessive dry biomass deposition found from the fouling experiments concerning *E.coli*. The inversion of the total interaction energy close to the wall can be explained by attractive electrostatic interactions due to an inversion of the logarithms in Eq. (11). These findings suggest that although often used in microbial systems, the X-DLVO might not be applicable for all microorganisms, experimental conditions and/or surfaces, but should rather be investigated more thoroughly as also suggested by Ninham et al. (2016) for complex interaction systems in general.

The classical DLVO theory was then also applied to the interaction system of Rhine microorganisms (with surface free energies according to Table 2 and the respective substrata with ion molarities of 0.0034 M according to Drever (1997) (see Fig. 5).

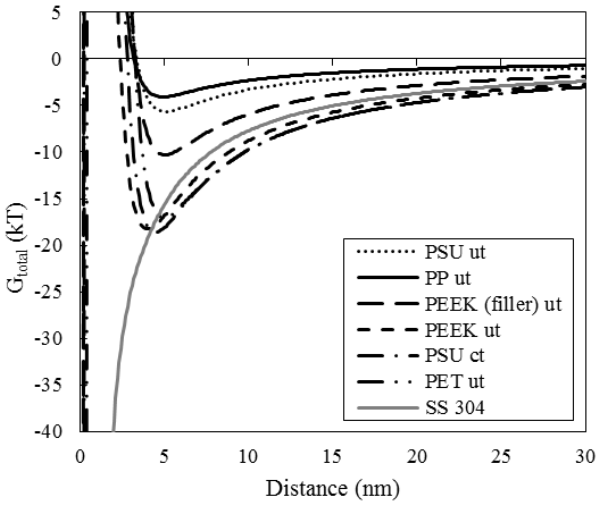

Fig. 4: Distance dependent interaction energies (DLVO) between E.coli K12 and the respective substrata, with ion molarities of 0.171 M according to the laboratory experiment at pH = 7

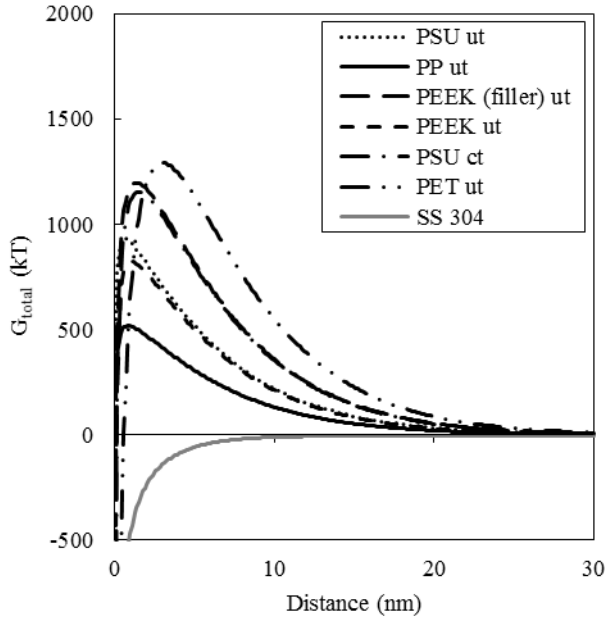

Fig. 5: Distance dependent interaction energies (DLVO) between Rhine microorganisms and the respective substrata, with ion molarities of 0.0034 M according to Drever (1997)

The mostly repulsive interaction energies of the polymers correlate qualitatively with the mean dry biomass according to Table 4, although no clear trends as in Fig. 4 could be observed. The SS 304 surface on the other hand shows attractive behavior across all separation distances due to the attractive Lifshitz-van der Waals forces and the negligible electrostatic interaction. These mainly attractive interaction energies are then reflected in the excessive dry biomass on SS 304 in contrast to the polymers by a factor of up to 12.

The results of applying the classical DLVO theory to complex autochthonous microorganisms in low-ionic systems and comparing them with experimental data suggest that valid fouling trends can be predicted for substrata with significant differing electrostatic properties as was given by

the neutral SS 304 in comparison to negatively charged polymers. The presence of possible hair-like cell appendages, which are commonly known for certain microorganisms, is not included in the DLVO theories. Especially concerning electrostatic interactions, the small radii of the cell appendage tips (see Eq. (11)) could lead to a bridging-effect circumventing the interaction of the larger microorganism with the substratum. This effect was not observed based on the data, as especially the used *E.coli* K12 tends to form few appendages but should be included in future investigations with other microorganisms.

Detachment wall shear stress

Fig. 6 shows the acquired wall shear stress for the respective substrata, which was necessary to detach the two week old biofilm, in relation to the acid-base fraction of the substrata surface free energy.

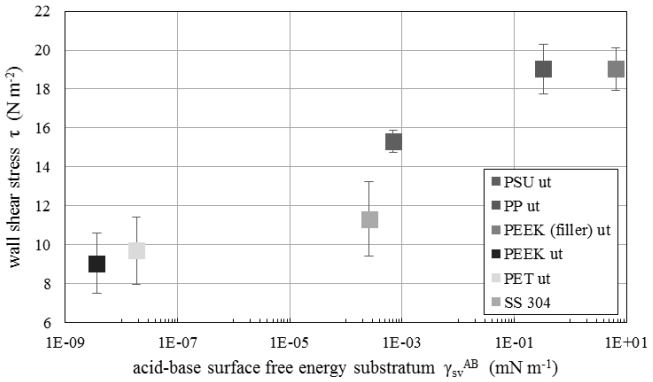

Figure 6: Measured wall shear stress to remove a two week old biofilm formed under laminar flow conditions in relation to the acid-base fraction of the surface free energy of the substrata

From Fig. 7 it can be seen, that the detachment wall shear stress seems to correlate with the acid-base fraction of the surface free energy. No other correlations of surface properties and wall shear stress could be found. This would mean, that a polar surface forms stronger adhesion forces between microorganism and substratum. Supporting evidence for these findings could be that the short-ranged polar forces influence adhesion in the wall-near region (e.g. Fig. 4), which was also investigated by other work groups (Krishnan et al. 2008; Banerjee et al. 2011). Nevertheless, an increased polarity of the surface would result in an increased repulsion based on the X-DLVO theory and therefore the adhesion itself would be governed by different processes than the near-wall interaction of microorganism and surface. It must also be mentioned, that the influence of cell appendages on the interaction and adhesion is scarcely investigated and neglected in most models (including DLVO and X-DLVO theory) but can have significant influence on the interaction process (Bos et al. 1999). As *E.coli* K12 DSM498 does not form cell appendages, this effect could be neglected in the interaction process towards the substrata and the interaction was therefore solely based on apolar and especially electrostatic forces as described in the classical DLVO theory.

CONCLUSIONS

The investigations of bacterial fouling on polymeric and stainless steel surfaces and the respective interaction forces performed in this study lead to the following conclusions:

1. An increase in bacterial cell numbers on the surface does not directly correlate with an increase of dry bacterial biomass. Data from the investigated polymers indicates the opposing behavior giving high bacterial cell numbers, but less dry biomass and vice versa.
2. The dry biomass of *E.coli* experiments are directly correlated with the apolar Lifshitz-van der Waals surface free energy fraction and the electrostatic interaction energies according to the classic DLVO theory. The X-DLVO including polar interaction energies was not able to reproduce the experimental data concerning dry biomass, especially for stainless steel. These data suggest further investigation of the applicability of the X-DLVO theory versus the DLVO theory.
3. Deposition of biomass was minimal for surfaces with apolar surface free energies of 25.29 mN m^{-1} for *E.coli* K12 DSM 498, which supports the findings of Zhao et al (2005) and Baier (1980). The same is true with 27.80 to 27.91 mN m^{-1} for autochthonous micro-organisms from Rhine and Moselle, respectively.
4. The dry biomass of autochthonous Rhine microorganisms in low-ionic systems could be qualitatively verified by using the classical DLVO theory and correlated to the excessive adhesion to SS 304 most likely due to its neutral electrostatic charge (IEP) at pH values of about 6.5 to 7.
5. The current DLVO and X-DLVO theories do not sufficiently reflect the presence of cell appendages and surface properties including roughness or conditioning films that are known to significantly influence the cell surface interaction.
6. Wall shear stresses between approximately 9 and 19 N m^2 were necessary to remove a laminar grown two week old biofilm of *E.coli* K12 from the investigated surfaces. Biofilms on PEEK ut showed minimal adhesion forces, whilst biofilms on PEEK (filler) ut were most resistant against detachment.
7. Further investigation concerning the biofilm characteristics like porosity and thickness are needed to correlate the findings concerning the dry biomass and fouling tendencies of each surface to its thermal impact.

NOMENCLATURE

A	surface area, m^2
A_H	Hamaker constant, J
ct	corona-treated
d	separation distance, m
d_h	characteristic length, 4 A_{flow}/U_{flow}, m
d_0	distance of closest approach, $1.58 \cdot 10^{-10}$ m, m
e	electron charge, 1.602177 10^{-19} C, C
G	interaction energies, J
ΔG_{adh}	adhesion energy, J m^{-2}
U	overall heat transfer coefficient, W m^{-2} K^{-1}

k	Boltzmann constant, 1.38064852 10^{-23} J/K, J/K
m	dry biomass, mg
n	cell numbers, (0.02 mm^2)$^{-1}$
n_i	number of ions per unit volume, -
p	probability value, -
r	radius, m
Re	Reynolds number, u d_h/ν, dimensionless
T	temperature, K
u	mean velocity, m s^{-1}
ut	untreated
x	height, m
z	valency of the ions, -

Greek Symbols

γ	surface free energy, mN m^{-1}
ε	dielectric constant of the liquid medium, F m^{-1}
ζ	zeta potential, mV
η	dynamic viscosity, Pa s
θ	contact angle, °
κ^{-1}	double layer thickness, m
λ_{th}	thermal conductivity, W m^{-1} K^{-1}
λ	correlation length, m
ν	kinematic viscosity, m^2s^{-1}
ρ	density, kg m^{-3}
τ	wall shear stress, N m^{-2}
ω	rotational speed, rad s^{-1}

Subscript and Superscript

AB	acid-base
adh	adhesion
d	disk
EL	electrostatic
f	fouling
l	liquid
LW	Lifshitz-van der Waals
m	microorganism
opt	optimal
s	solid
v	vapor
0	initial condition
+	electron acceptor
-	electron donor

REFERENCES

Baier, R.E., 1980, Adsorption of Microorganisms to Surface. New York, USA; Wiley-Interscience Publishers, pp. 59-104.

Banerjee, I., Pangule, R.C., Kane, R.S., 2011, Antifouling Coatings: Recent Developments in the Design of Surfaces that Prevent Fouling by Proteins, Bacteria and Marine Organisms. Adv. Mater., Vol. 23, pp. 690-718.

Bos, R., van der Mei, H.C., Busscher, H.J., 1999, Physico-chemistry of initial microbial adhesive interactions – its mechanisms and methods for study. FEMS Microbiol. Reviews, Vol. 23, pp. 179-230.

Derjaguin, B., Landau, L., 1941, Theory of the stability of strongly charged lyophobic sols and of the adhesion of strongly charged particles in solutions of electrolytes. Acta Physico Chemica URSS. Vol. 14, pp. 30–59.

Drever, J.I., 1997, The Geochemistry of Natural Waters: Surface and Groundwater Environments. New Jersey, USA; Prentice Hall. ISBN 978-0132727907.

Fowler, H.W., McKay, A.J., 1980, The measurement of microbial adhesion. In: Berkeley R.C.W. et al., (eds.) in: Microbial adhesion to surfaces. Chichester, UK; Ellis Horwood Ltd, pp. 141-163.

García, A.J., Ducheyne, P., Boettinger, D., 1997, Quantification of cell adhesion using a spinning disc device and application to surface-reactive materials, Biomater., Vol. 18, pp. 1091-1098.

Krishnan, S., Weinman, C.J., Ober, C.K., 2008, Advances in polymers for anti-biofouling surfaces. J. Mater. Chem., Vol. 18, pp. 3405-3413.

Luxbacher, T., 2014, The Zeta potential for solid surface analysis: a practical guide to streaming potential measurement. Graz, Austria; Anton Paar GmbH, ISBN: 9783200035539.

Ninham, B. W., Pashley, R. M. Lo Nostro, P., 2017, Surface forces: Changing concepts and complexity with dissolved gas, bubbles, salt and heat, Curr. Opin. Colloid Interface Sci., Vol. 27, pp. 25-32.

Pohl, S., Madzgalla, M., Manz, W. and Bart, H.-J., 2015a, Biofilm formation on Polymeric Heat Transfer Surfaces, Proceedings of the International Conference on Heat Exchanger Fouling and Cleaning XI, p. 231-235.

Pohl, S., Madzgalla, M., Manz, W. and Bart, H.-J., 2015b, Biofouling on polymeric heat exchanger surfaces with *E.coli* and native biofilms, Biofouling, Vol. 31, pp. 699-707.

Pohl, S., Madzgalla, M., Manz, W. and Bart, H.-J., 2017, *E.coli* biofilm characteristics on polymeric heat exchanger surfaces, Chem. Eng. Technol., Vol. 40(6), pp. 1017-2014.

Schlichting, H., Gersten, K., 2000, Boundary layer theory, 8th edition, Berlin, Deutschland; Springer-Verlag.

Soni, K.A., Balasubramanian, A.K., Beskok, A., Pillai, S.D., 2007, Zeta Potential of Selected Bacteria in Drinking Water When Dead, Starved or Exposed to Minimal and Rich Culture Media. Curr. Microbiol., Vol. 56, pp. 93-97.

Tan, C.H., Koh, K.S., Xie, C., Tay, M., Zhou, Y., Williams, R., Ng, W.J., Rice, S.A., Kjelleberg, S., 2014, The role of quorum sensing signaling in EPS production and the assembly of a sludge community into aerobic granules. ISME J., Vol. 8, pp. 1186-1197.

Verwey, E. J. W., Overbeek, J. Th. G., 1948, Theory of the stability of lyophobic colloids. Elsevier, New York.

van Oss, C.J., 1995, Hydrophobicity of biosurfaces – origin, quantitive determination and interaction energies. Colloids Surf. B. Vol. 5, pp. 91-110.

Wilson, W.W., Wade, M.M., Holman, S.C., Champlin, F.R., 2001, Status of methods for assessing bacterial cell surface charge properties based on zeta potential measurements. J. Microbiol. Methods, Vol. 43, pp. 153-164.

Zhao, Q., Liu, Y., Wang, C., Wang, S., Müller-Steinhagen, H., 2005, Effect of surface free energy on the adhesion of biofouling and crystalline fouling. Chem. Eng. Sci., Vol. 60, pp. 4858-4865.